

Surface-electronic structure of La(0001) and Lu(0001)

D. Wegner,¹ A. Bauer,¹ Yu. M. Koroteev,^{2,3} G. Bihlmayer,⁴ E. V. Chulkov,^{2,5} P. M. Echenique,^{2,5} and G. Kaindl¹

¹*Institut für Experimentalphysik, Freie Universität Berlin, Arnimallee 14, 14195 Berlin-Dahlem, Germany*

²*Donostia International Physics Center (DIPC), Paseo de Manuel Lardizabal 4, 20018 San Sebastián/Donostia, Basque Country, Spain*

³*Institute of Strength Physics and Material Science, Russian Academy of Sciences, 634021 Tomsk, Russia*

⁴*Institut für Festkörperforschung, Forschungszentrum Jülich, D-52425 Jülich, Germany*

⁵*Departamento de Física de Materiales and Centro Mixto CSIS-UPV/EHU, Facultad de Ciencias Químicas, UPV/EHU, Apdo. 1072, 20080 San Sebastián/Donostia, Basque Country, Spain*

(Dated: November 17, 2005)

Most spectroscopic methods for studying the electronic structure of metal surfaces have the disadvantage that either only occupied or only unoccupied states can be probed, and the signal is cut at the Fermi edge. This leads to significant uncertainties, when states are very close to the Fermi level. By performing low-temperature scanning tunneling spectroscopy and *ab initio* calculations, we study the surface-electronic structure of La(0001) and Lu(0001), and demonstrate that in this way detailed information on the surface-electronic structure very close to the Fermi energy can be derived with high accuracy.

PACS numbers: 73.20.At, 71.20.Eh, 73.50.Gr, 68.37.Ef, 71.15.Mb

After the first theoretical prediction of a Tamm-like surface state on Gd(0001) [1], surface states with d_{z^2} symmetry around the center of the surface Brillouin zone (BZ) have been found on all trivalent lanthanide metals by photoemission (PE) and inverse photoemission (IPE) [2, 3, 4, 5, 6, 7]. In all cases, the surface state was found to be located very close to the Fermi energy, E_F , where the accuracy of these experimental methods deteriorates due to the signal cutoff at E_F . This weakness is manifested in the case of Gd(0001): First, a combined PE and IPE study concluded that the exchange splitting of the surface state decreases with increasing temperature and vanishes within experimental accuracy above the Curie temperature (T_C) [8]; later, a scanning tunneling spectroscopy (STS) study showed that in fact a constant residual splitting persists above T_C [9]. This was the first striking demonstration that STS is a very sensitive technique when states are located very close to E_F , because both occupied and unoccupied states can be probed within a single measurement, without any influence on the spectroscopic signal when crossing E_F . Consequently, recent systematic studies of magnetic lanthanide metals across the whole series of lanthanide metals demonstrated that STS at low temperatures can probe these surface states with unprecedented accuracy [10, 11, 12].

Here, we focus on the nonmagnetic $4f$ metals La and Lu. In both cases, PE and IPE could not clarify whether the binding energy at the center of the BZ, $\bar{\Gamma}$, is below or above E_F . While for Lu(0001) only PE data exists [7, 13], a combined PE and IPE study of La(0001) concluded that the surface state is partially occupied [5]. However, due to the total system resolution in these experiments, the reliability of this latter statement must be considered to be questionable. Furthermore, theoretical band

structures are not available for La(0001) and Lu(0001) up to now. We therefore performed low-temperature STS studies and band-structure calculations for these two lanthanide surfaces. In the present work, we compare the theoretical and experimental results, and we show that – with the help of the calculated surface-band structure – the STS data can be described accurately by simple models which do not only yield surface-state binding energies but also lifetime widths and the dispersion of the surface bands.

The experiments were performed in an ultrahigh vacuum (UHV) chamber equipped with a low-temperature STM operated at 10 K [10]. The samples were prepared *in situ* by vacuum deposition of electron-beam-evaporated La or Lu metal (≈ 30 ML), respectively, on a clean W(110) single crystal substrate followed by annealing at 800 K in case of La and 1000 K in case of Lu. STM images were taken in constant-current mode, and the STS spectra were recorded with fixed tip position, i.e. open feedback loop. The tunneling current I and the differential conductivity, dI/dV , were recorded as a function of sample bias voltage, V , by modulating V and recording the induced modulation of I via lock-in technique. A modulation amplitude of 1 mV (rms) at a frequency of ≈ 360 Hz was used, with the time constant of the lock-in amplifier set between 10 and 100 ms, at a sweep rate of ≈ 2 mV/s. The spectra were taken in both directions, from lower to higher and from higher to lower sample bias, in order to verify that energy shifts (due to the finite time constant) are below 1 meV. Since both the STM tip and the sample were cooled to 10 K, the energy resolution was ≈ 3 meV, corresponding to $3.5k_B T$.

The calculations were performed using density functional theory (DFT) in the generalized gradient approximation (GGA) as given by Perdew and Wang [14]. We

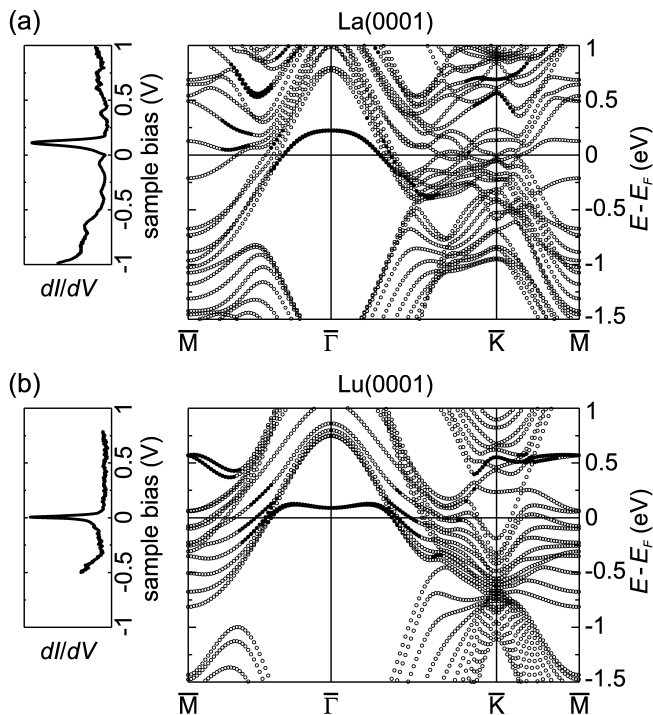


FIG. 1: (a) Tunneling spectrum of La(0001) at $T = 10$ K (rotated) and calculated band structure of a relaxed 11 layer La(0001) film. Surface states are marked by filled circles, bulk states by open circles. The most pronounced peak in the STS data at around 0.1 eV is attributed to the narrow surface-state band around the $\bar{\Gamma}$ point of the surface Brillouin zone. (b) Tunneling spectrum of Lu(0001) at $T = 10$ K and corresponding band structure of a relaxed 12 layer Lu(0001) film. The surface state appears as a sharp peak at E_F in STS.

use the full-potential linearized augmented plane-wave method in film geometry [15, 16] as implemented in the FLEUR code [17]. Spin-orbit coupling is induced self-consistently as described in Ref. 18. For a proper description of the $4f$ electrons, we apply the LDA+U method [19] in an implementation similar to that of Shick *et al.* [20]. For La, we used values of $U = 8.1$ eV and $J = 0.6$ eV, for Lu of $U = 4.8$ eV and $J = 0.95$ eV. These parameters were chosen to simulate the experimentally observed positions of the $4f$ bands [21]. The La(0001) surface was simulated by an 11-layer film embedded in semi-infinite vacua, for the Lu(0001) surface a 12-layer film was used. The vacuum region was chosen to start 3.2 a.u. and 2.9 a.u., respectively, above the surface atoms of La and Lu. The muffin-tin spheres had a radius of 3.0 a.u. in case of La and 2.8 a.u. in case of Lu. A plane-wave cutoff of $K_{\max} = 3.4$ (a.u.) $^{-1}$ was used, and the irreducible part of the two-dimensional BZ was sampled with 21 special k_{\parallel} points.

In Fig. 1(a), the STS spectrum of La(0001) is shown (rotated by 90°), together with the calculated band structure. The "overview" spectrum is dominated by a narrow peak at $V \approx 0.1$ V which is the signature of the d_{z^2} -like

surface state. As STS probes mainly states around the $\bar{\Gamma}$ point of the projected surface BZ, the interpretation of the peak as a surface state is clearly confirmed by the band structure calculation, where a narrow downward-dispersing surface-state band is clearly visible in the local gap around $\bar{\Gamma}$ at about 0.2 eV above E_F . Fig. 1(b) displays the STS data and corresponding calculated band structure of Lu(0001). Again, the only feature in STS is a sharp peak located close to $V = 0$ (i.e. $E = E_F$). It can be identified as the surface state by comparison with the band structure, which shows a surface state at 90 meV.

A comparison of the band structures of La(0001) and Lu(0001) with those of other lanthanide metals shows that their electronic structures around $\bar{\Gamma}$ are very similar, i.e. only small systematic changes occur across the lanthanide series. A clear trend in the band dispersion is visible: While for La, the effective mass is negative (i.e. the dispersion is downward towards lower energies $E - E_F$), Lu first shows a weak upward dispersion at $\bar{\Gamma}$, which changes to downward with a band maximum at $\approx 1/4$ way towards the BZ boundary. The dispersion of Gd is "in between" with a very flat surface-state band [22]. Calculations for Ce and Tm confirm this trend [6, 23]. This systematic change further leads to a decrease of the surface-state bandwidth and higher effective masses across the lanthanide series. From Fig. 1, $|m^*/m| > 2$ for La and $|m^*/m| > 5$ for Lu can be estimated. Experimentally, in another STS study of Gd, Ho, and Lu we estimated $|m^*/m| > 5$ [10]; a recent PE study of Ce concludes that $|m^*/m| \approx 7.4$ [23]. These large effective masses are the result of the high degree of lateral localization of the Tamm-like lanthanide-surface states. Consequently, they appear as peaks in STS rather than as step-like functions (as would be expected for delocalized Shockley-like surface states, e.g. on the (111) surfaces of the noble metals).

For a quantitative analysis of the spectral shape of the surface states in STS, we have applied a fit analysis that is based on planar tunneling theory [24]. The fit model was already introduced in Ref. 10. Therefore, we shall only briefly summarize it here. Assuming that the DOS of the tip is constant (within the energy range of interest) and that the transmission coefficient for tunneling, $T(E)$, is bias-independent (for small V), the differential conductivity is given by

$$\frac{dI}{dV} \propto \int_{-\infty}^{+\infty} (n_s T)(E) f'(E - eV) dE, \quad (1)$$

where n_s is the DOS of the sample, and f' is the derivative of the Fermi-distribution function; the latter takes into account the thermal broadening of the spectra due to the finite temperature in the experiment. For a surface band with quadratic dispersion, $E(k_{\parallel}) = E_0 + (\hbar^2/2m^*)k_{\parallel}^2$, and negative effective mass ($m^* < 0$), the DOS is a step function: $n_s \propto \theta(E_0 - E)$. Furthermore, assuming $|m^*| \ll m$ and $E_{\perp} = E - E_{\parallel} < \phi_{\text{eff}}$, T

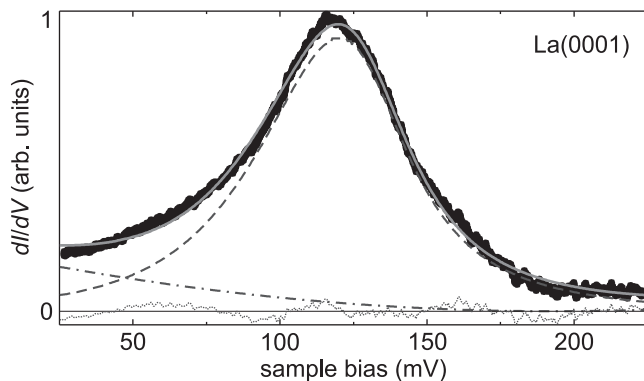


FIG. 2: Highly resolved tunneling spectrum of La(0001) at $T = 10$ K and least-squares fit (grey line) composed of a surface-state line according to Eq. 1 to 3 (dashed) and a quadratic background (dash-dotted) to account for tunneling into bulk states. The residual of the fit is shown as a thin dotted line.

can be approximated as:

$$\begin{aligned} T(E) &= \exp\left(-2z\sqrt{\frac{2m}{\hbar^2}(\phi_{\text{eff}} - E_{\perp})}\right) \\ &= \exp\left(-2z\sqrt{\frac{2m}{\hbar^2}(\phi_{\text{eff}} - E) + k_{\parallel}^2}\right) \\ &\propto \exp[-p_1(E_0 - E)], \end{aligned} \quad (2)$$

where ϕ_{eff} is the effective barrier height, z is the tip-sample distance, and E_{\perp} is the perpendicular energy component. p_1 is a constant parameter, with $p_1 = z\sqrt{2m/\hbar^2\phi_{\text{eff}}}(m^*/m)$ [10]. Thus, the important term in Eq. 1, $n_s T$, is simply an exponential function that is cut at the band maximum E_0 by the step function.

To account for finite lifetimes, each contributing state of the surface band is broadened by a Lorentzian function. This is realized by writing $n_s T$ as an integral over Lorentzians weighted with T :

$$n_s T(E) \propto \int \frac{\Gamma(\varepsilon)}{(E-\varepsilon)^2 + (\Gamma(\varepsilon)/2)^2} \times \theta(E_0 - \varepsilon) \exp[-p_1(E_0 - \varepsilon)] d\varepsilon. \quad (3)$$

Γ is the full width at half maximum of the Lorentzian, which is related to the lifetime τ by $\Gamma = \hbar/\tau$. Γ is written as a function of energy in order to account for possible energy dependences of the lifetime due to electron-electron (e - e) and electron-phonon (e -ph) scattering [25, 26, 27, 28].

In summary, this model reflects the influence of band dispersion which leads to slightly asymmetric peaks with broad leading and narrow trailing edges. Although the above approximations are not valid for a strongly dispersing band, this model can be qualitatively conveyed into the model of Li *et al.*, who analyzed the width of the Ag(111) surface-state spectrum [29]. While a large p_1 factor (due to a high effective mass) leads to narrow peaks in STS, a small m^* (as for the sp -like surface states of the noble metals) would result in a small p_1 . So the

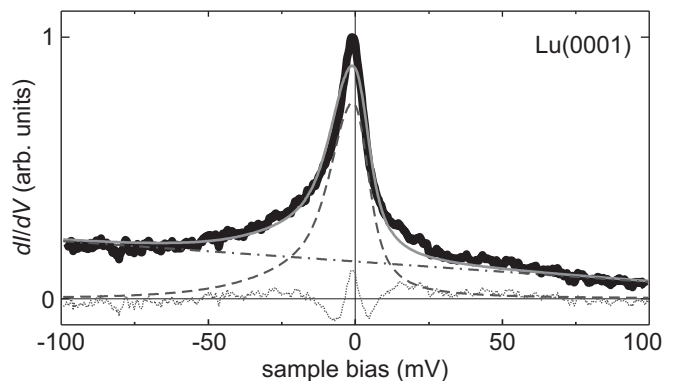


FIG. 3: Highly resolved tunneling spectrum of Lu(0001) at $T = 10$ K and least-squares fit (grey line) composed of a surface-state line according to Eq. 1 to 3 (dashed) and a quadratic background (dash-dotted) to account for tunneling into bulk states. The residual of the fit is shown as a thin dotted line.

exponential decrease of the STS signal becomes negligible, and a step function remains which is broadened by Lorentzians (corresponding to an arctan function, as in Ref. 29). Indeed, on a larger energy scale also in tunneling spectra of the surface states on the (111) faces of noble metals a deviation from a step function can be observed in the form of a weak decrease of dI/dV towards higher energies [30, 31].

In Fig. 2, a highly resolved tunneling spectrum is plotted together with the results of the fit analysis. As can be seen from the residual, the fit describes the experimental curve very well. This confirms that – for Gd, Tb, Dy, Ho, and Er [10, 12] – the applied model works convincingly for a monotonically downward-dispersing surface state with high effective mass. According to the fit result, the band maximum is located at $E_0 = (130 \pm 5)$ meV, and the lifetime width at the band maximum is $\Gamma(E_0) = (49 \pm 10)$ meV, which corresponds to a lifetime of $\tau(E_0) = (13 \pm 3)$ fs. Thus, the band is clearly unoccupied at $\bar{\Gamma}$ and crosses the Fermi level at about 1/4 way towards the BZ boundary. The experimental value for the band maximum is about 70 meV below the theoretical one. As can be seen in the comparison with Ce(0001) [23], Gd(0001) [22], and Lu(0001) (see below), DFT calculations of the unoccupied lanthanide-surface states always yield slightly higher energies for the band maximum.

In the following discussion, we compare the results with literature. A combined PE and IPE study of La(0001) showed that the surface state is partially occupied at $\bar{\Gamma}$ at room temperature [5, 32]. As this is clearly not the case in the present STS study at 10 K, the former observation can only be explained as a temperature effect in two ways: (i) The surface-state band may shift down with temperature. However, we have also applied STS on La(0001) at $T \approx 60$ K and did not see any shift of the band maximum. Therefore, we exclude

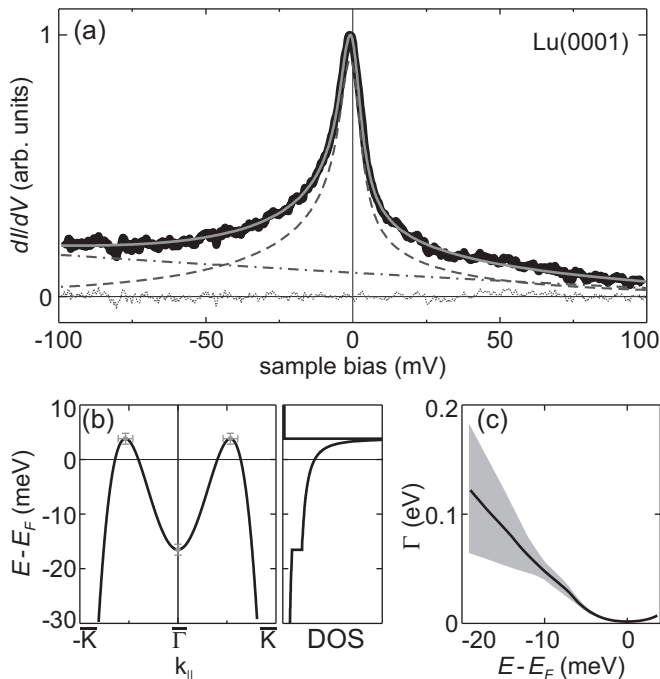


FIG. 4: (a) Same tunneling spectrum of Lu(0001) as in Fig. 3. The grey line represents a least-squares fit composed of a surface-state line according to the new model (Eq. 7) (dashed) and a quadratic background (dash-dotted) to account for tunneling into bulk states. The residual of the fit is shown as a thin dotted line. (b) Dispersion and density of states (DOS) of the Lu-surface band, and (c) energy-dependent lifetime width resulting from the fit analysis.

this possibility. (ii) The linewidth increases with temperature, and thereby the surface state protrudes over the Fermi edge and becomes partially occupied. Our analysis of the spectrum at 60 K shows an increase of the linewidth by ≈ 20 meV. In first approximation, the linewidth increases linearly with temperature due to enhanced electron-phonon scattering [25, 27]. By extrapolation, the linewidth at room temperature is estimated to be at least 0.2 eV, i.e. mechanism (ii) explains the different results of this study and of Ref. 5 as a temperature effect. Furthermore, taking into account the IPE energy resolution of ≈ 0.2 eV, it is clear that no statement on the exact position of the band maximum could have been made in Ref. 5. The comparison with our results points out the advantage of STS, which simultaneously probes both occupied and unoccupied states around E_F .

Fig. 3 shows a highly resolved tunneling spectrum of Lu(0001) plotted together with the least-squares fit results. In this case, the residual illustrates that the fit model does not sufficiently well describe the experimental data. As pointed out recently [10], the fit model works only satisfactorily for Lu(0001), if an additional Gaussian function is added to describe both the broad tails and the sharp peak in the spectrum. At present there is, however, no clear physical explanation for such an addi-

tional feature, thus this procedure is questionable. The model curves in Fig. 3 show the fit result without such a Gaussian function to emphasize the deviations.

An inspection of the results of the band-structure calculation [Fig. 1(b)] explains why the above model, which assumes a monotonic downward dispersion of the surface band, could not be successful, because the Lu surface band follows a more complicated dispersion. The band maximum at $k_{\parallel} \neq 0$ leads to a singularity in the DOS that must be taken into account, and also the energy dependence of the tunneling probability is different for such an M-shaped surface band. Therefore, we introduce a more sophisticated model to describe the lineshape of the STS data.

The simplest extension of the former model is to assume a parabolic dispersion of 4th order, $E(k_{\parallel}) = E_0 + ak_{\parallel}^2 + bk_{\parallel}^4$, with $a > 0$ and $b < 0$; with this ansatz, $E(k_{\parallel} = 0) = E_0$ is the local band minimum at $\bar{\Gamma}$. The band maximum is located at $k_{\max} = \sqrt{-a/2b}$ and has the energy $E_{\max} = E_0 + \Delta E$, where $\Delta E = -a^2/4b$. Thus, a and b can be exchanged by the more descriptive parameters k_{\max} and ΔE :

$$E(k_{\parallel}) = E_0 + 2\Delta E(k_{\parallel}/k_{\max})^2 - \Delta E(k_{\parallel}/k_{\max})^4. \quad (4)$$

For $|k_{\parallel}| \geq k_{\max}$, this results in

$$|k_{\parallel}(E)| = k_{\max} \left(1 \pm \sqrt{1 + \frac{E_0 - E}{\Delta E}} \right)^{1/2}, \quad (5)$$

and the DOS of the surface band can be calculated as:

$$n_s \propto k_{\parallel} \left| \frac{dk_{\parallel}}{dE} \right| = \left| \frac{k_{\max}^2}{4\Delta E \sqrt{1 + \frac{E_0 - E}{\Delta E}}} \right|. \quad (6)$$

As the dispersion in this model is not simply quadratic, the approximation for the transmission coefficient in Eq. 2 is not valid anymore, and the general formula must be used.

For $E_0 < E < E_{\max}$, two solutions exist, i.e. for the same energy there are two contributions to the tunneling current with different momentum $k_{\parallel}^{(a)} < k_{\max}$ and $k_{\parallel}^{(b)} > k_{\max}$, respectively. This can be included by a sum of two transmission coefficients T_a and T_b . For $E < E_0$, T_a is set to zero.

Finally, as for the above model, the broadening of each state due to the finite lifetime is included by an integral over Lorentzian functions:

$$\frac{dI}{dV} = p_0 \int \int \frac{\Gamma(\epsilon)}{(E-\epsilon)^2 + (\frac{\Gamma(\epsilon)}{2})^2} n_s(E) \times [T_a(E) + T_b(E)] f'(E - eV) d\epsilon dE. \quad (7)$$

In summary, the fit routine possesses the free parameters: E_0 , ΔE , k_{\max} , Γ , ϕ_{eff} , and z . At a first glance, this number seems to be too large for a reasonable fit. However, due to the knowledge of the band dispersion from

Fig. 1(b), ΔE and k_{\max} can be restricted to a region that is compatible with the calculated band structure. Also the last two parameters can be limited because the barrier height should not differ much from the work function of Lu (≈ 3.3 eV), and the typical tip-sample distance is between 5 and 15 Å.

For Γ , we take into account the energy dependence due to e -ph scattering ($\Gamma_{e\text{-ph}}$) according to the Debye model [25, 33, 34], and the quadratic energy dependence due to e - e scattering ($\Gamma_{e\text{-}e} = 2\beta[(\pi k_B T)^2 + (E - E_F)^2]$) as described by Fermi-liquid theory [26, 35]. $\Gamma_{e\text{-ph}}$ is determined by the e -ph mass enhancement parameter λ and the Debye energy $\hbar\omega_D$. $\Gamma_{e\text{-}e}$ is described by the parameter 2β [11]. Further, an offset Γ_0 is used as additional parameter in order to include the possibility that $\Gamma(E_F) > 0$. Thus, the lifetime width is only considered to be energy-dependent in this model but not k_{\parallel} -dependent. We point out that also a momentum dependence is to be expected, caused e.g. by interband e - e scattering with bulk bands, which is more probable when the excited state is further away from the center of the BZ. However, including these effects requires a much more complicated model [28, 36] and is beyond the scope of this study.

Fig. 4(a) displays the result of a fit analysis of the same Lu(0001) tunneling spectrum as shown in Fig. 3, but now with the new fit model. As can be seen from the residual, the model curve fits the experimental data perfectly. The results for the fit parameters are listed in Tab. I. In order to test the reliability of the model, several STS spectra were fitted, and the reasonability of the parameters was checked. Although these parameters were treated as free parameters in the fit procedure, they were found to vary only slightly. Some values that deviate from the expected values of the calculation will be discussed in the following. However, the qualitative agreement is good enough to specify the dispersion of the surface band, cf. Fig. 4(b).

Comparison with the calculated band structure in Fig. 1(b) gives good compliance in ΔE , while the energy position of the band – as discussed above – is again too high in the DFT calculation in GGA approximation. The difference in k_{\max} is large. While theory puts it to one fourth, the band maximum in the fit is at about one half of the surface BZ, where the band structure is already dominated by bulk bands. Probably, the k_{\parallel} dependence of the fit is quantitatively incorrect, which is not unexpected since the model is based on planar tunneling theory. The DOS of the M-shaped surface band [Fig. 4(b)], however, shows that – due to the singularity at E_{\max} – states away from $\bar{\Gamma}$ have a dominant influence on the lineshape of the tunneling spectrum. Thus, the Lu(0001) surface band is occupied at the center of the surface BZ, but it has much more unoccupied DOS slightly above E_F . Due to its unique dispersion, the surface band crosses the Fermi edge twice. The parameters ϕ_{eff} and z vary barely. A tip-sample distance of 11 Å is realistic. The effective work function may be slightly too small but is still in a reasonable regime.

For an estimation of the energy dependence of Γ , all

relevant parameters have been set free in the fit procedure. The small offset $\Gamma_0 = \Gamma(E_F) = (2 \pm 1)$ meV can be explained either by a small contribution of defect scattering or by a poorer experimental resolution (maybe due to electronic noise). At the band maximum, the lifetime width is $\Gamma(E_0 + \Delta E) = (8 \pm 2)$ meV. The parameters for e -ph scattering are again acceptable: $\lambda = 1.4 \pm 0.9$ is higher than the calculated value of Skriver *et al.* [37], but also other experiments find larger electron-phonon mass enhancement factors up to 2.1 [38]. The Debye energy, according to the fit result, is $\hbar\omega_D = (12 \pm 4)$ meV, which is between the bulk value of 15.8 meV and the recently determined value for the surface-Debye energy of 10.4 meV [7].

In contrast, the values describing e - e scattering are rather unprecise, particularly for $E_F - E > 10$ meV. The 2β parameter varies between 0 and (unphysical) 100 eV $^{-1}$ for different tunneling spectra. For a clearer validation, the mean value of Γ is plotted versus the energy [Fig. 4(c)], the grey-shaded area marks the uncertainty region. In the relevant region ± 10 meV around E_F , where the surface-state peak occurs in STS, the variation of $\Gamma(E)$ is relatively small. Only for lower energies $E_F - E > 10$ meV, where the contribution of the surface state to the STS signal decreases rapidly, the determination of the linewidth becomes untrustworthy, and the error bars get accordingly very large. In the spectroscopically crucial region, however, the error bars are smaller than 10 meV. To further test the model, the 2β factor was fixed to realistic values (between 0 and 1 eV $^{-1}$), and the fit procedure was applied only within the relevant region of the STS spectra. The resulting parameters do not deviate significantly from those in Tab. I, which emphasizes that the lineshape is predominantly caused by the unusual DOS of the M-shaped surface band.

We point out again that the difficulties in deriving precise values for the linewidth may be due to the fact that the model does not contain a k_{\parallel} -dependence of Γ . For instance, the e - e scattering rate for an excited hole at the $\bar{\Gamma}$ point, i.e. deep within the local band gap, is predominantly determined by intraband relaxation pro-

TABLE I: Parameters resulting from the fit analysis of the Lu(0001) STS data according to the new model. For comparison, the "starting" values expected from calculations are also listed.

parameters	fit result	"starting" values
E_0 (meV)	-17 ± 2	90
ΔE (meV)	20.3 ± 0.3	34
k_{\max} (Å $^{-1}$)	0.64 ± 0.09	0.27
ϕ_{eff} (eV)	2.11 ± 0.05	3.3
z (Å)	10.9 ± 0.5	5...15
Γ_0 (meV)	2 ± 1	0
λ	1.4 ± 0.9	0.59
$\hbar\omega_D$ (meV)	12 ± 4	15.8
2β (eV $^{-1}$)	0...100	< 1

cesses, while for an excited hole with the same energy E_0 at the decreasing part of the surface band, additional interband transitions into nearby bulk bands are possible. The interplay between intra- and interband scattering can be complicated, even for relatively simple systems as the noble metals [28, 36]. Also, in case of the far more complex surface state of Lu(0001), only elaborate calculations will allow for a quantitative understanding of surface-state dynamics. Given the current state of the art, the new expanded model can be rated as a useful description for the STS data of Lu(0001).

In summary, we have presented low-temperature scanning-tunneling spectroscopy data and density-functional calculations for the (0001) surfaces of La and Lu. Fit analyses of the spectra yield quantitative information about the surface-band dispersions and the electronic lifetimes of the surface states. The surface state

at the BZ center of La(0001) is clearly unoccupied, but crosses E_F due to a downward dispersion towards the BZ boundary. The surface band of Lu exhibits an M-shaped dispersion, with an occupied local minimum at $\bar{\Gamma}$ and an off-centered band maximum slightly above E_F . We demonstrated that STS results for Lu(0001) can be described well by an extended – but still rather simple – model. We conclude that STS in combination with *ab initio* calculations enables one to obtain detailed information with high accuracy on the surface-electronic structure of metals near the Fermi energy.

This work was supported by the Deutsche Forschungsgemeinschaft (DFG), projects Sfb-290/TPA6 and KA 564/10-1, and by the University of the Basque Country, Departamento de Educación del Gobierno Vasco and MCyT (Grant No. MAT 2001-0946). A.B. acknowledges support within the Heisenberg program of the DFG.

-
- [1] R. Wu, C. Li, A. J. Freeman, and C. L. Fu, Phys. Rev. B **44**, 9400 (1991).
- [2] D. Li, C. W. Hutchings, P. A. Dowben, C. Hwang, R.-T. Wu, M. Onellion, A. B. Andrews, and J. L. Erskine, J. Magn. Magn. Mater. **99**, 85 (1991).
- [3] S. C. Wu, H. Li, Y. S. Li, D. Tian, J. Quinn, F. Jona, and D. Fort, Phys. Rev. B **44**, 13720 (1991).
- [4] S. S. Dhesi, R. I. R. Blyth, R. J. Cole, P. A. Gravil, and S. D. Barrett, J. Phys.: Condens. Matter **4**, 9811 (1992).
- [5] A. V. Fedorov, A. Höhr, E. Weschke, K. Starke, V. K. Adamchuk, and G. Kaindl, Phys. Rev. B **49**, R5117 (1994).
- [6] M. Bodenbach, A. Höhr, C. Laubschat, G. Kaindl, and M. Methfessel, Phys. Rev. B **50**, 14446 (1994).
- [7] E. Weschke and G. Kaindl, J. Electron Spectrosc. Relat. Phenom. **75**, 233 (1995).
- [8] E. Weschke, C. Schüßler-Langeheine, R. Meier, A. V. Fedorov, K. Starke, F. Hübing, and G. Kaindl, Phys. Rev. Lett. **77**, 3415 (1996).
- [9] M. Bode, M. Getzlaff, S. Heinze, R. Pascal, and R. Wiesendanger, Appl. Phys. A **66**, S121 (1998).
- [10] A. Bauer, A. Mühlig, D. Wegner, and G. Kaindl, Phys. Rev. B **65**, 75421 (2002).
- [11] A. Rehbein, D. Wegner, G. Kaindl, and A. Bauer, Phys. Rev. B **67**, 33403 (2003).
- [12] A. Bauer, D. Wegner, and G. Kaindl, cond-mat/0502581 (2005).
- [13] G. Kaindl, A. Höhr, E. Weschke, S. Vandr e, C. Schüßler-Langeheine, and C. Laubschat, Phys. Rev. B **51**, 7920 (1995).
- [14] J. P. Perdew, J. A. Chevary, S. H. Vosko, K. A. Jackson, M. R. Pederson, D. J. Singh, and C. Fiolhais, Phys. Rev. B **46**, 6671 (1992).
- [15] E. Wimmer, H. Krakauer, M. Weinert, and A. J. Freeman, Phys. Rev. B **24**, 864 (1981).
- [16] M. Weinert, E. Wimmer, and A. J. Freeman, Phys. Rev. B **26**, 4571 (1982).
- [17] URL <http://www.flapw.de>.
- [18] C. Li, A. J. Freeman, H. J. F. Jansen, and C. L. Fu, Phys. Rev. B **42**, 5433 (1990).
- [19] V. L. Anisimov, F. Aryasetiawan, and A. I. Lichtenstein, J. Phys.: Condens. Matter **9**, 767 (1997).
- [20] A. B. Shick, A. I. Liechtenstein, and W. E. Pickett, Phys. Rev. B **60**, 10763 (1999).
- [21] J. K. Lang, Y. Baer, and P. A. Cox, J. Phys. F: Metal Phys. **11**, 121 (1981).
- [22] P. Kurz, G. Bihlmayer, and S. Blügel, J. Phys. Condens. Matter **14**, 6353 (2002).
- [23] F. Schiller, M. Heber, V. D. P. Servedio, and C. Laubschat, Phys. Rev. B **68**, 233103 (2003).
- [24] E. L. Wolf, *Principles of Electron Tunneling Spectroscopy* (Oxford, New York, 1985).
- [25] G. Grimvall, *The Electron-Phonon Interaction in Metals* (North-Holland, New York, 1981).
- [26] J. J. Quinn, Phys. Rev. **126**, 1453 (1962).
- [27] B. Hellsing, A. Eiguren, and E. V. Chulkov, J. Phys.: Condens. Matter **14**, 5959 (2002).
- [28] P. M. Echenique, R. Berndt, E. V. Chulkov, T. Fauster, A. Goldmann, and U. Höfer, Surf. Sci. Rep. **52**, 219 (2004).
- [29] J. Li, W.-D. Schneider, R. Berndt, O. R. Bryant, and S. Crampin, Phys. Rev. Lett. **81**, 4464 (1998).
- [30] J. Li, W.-D. Schneider, S. Crampin, and R. Berndt, Surf. Sci. **422**, 95 (1999).
- [31] L. Limot, T. Maroutian, P. Johansson, and R. Berndt, Phys. Rev. Lett. **91**, 196801 (2003).
- [32] E. Weschke, A. Höhr, G. Kaindl, S. L. Molodtsov, S. Danzenb acher, M. Richter, and C. Laubschat, Phys. Rev. B **58**, 3682 (1998).
- [33] B. A. McDougall, T. Balasubramanian, and E. Jensen, Phys. Rev. B **51**, R13891 (1995).
- [34] E. V. Chulkov, J. Kliewer, R. Berndt, V. M. Silkin, B. Hellsing, S. Crampin, and P. M. Echenique, Phys. Rev. B **68**, 195422 (2003).
- [35] D. Pines and P. Nozi eres, *The Theory of Quantum Liquids* (Benjamin, New York, 1969).
- [36] L. Vitali, P. Wahl, M. A. Schneider, K. Kern, V. M. Silkin, E. V. Chulkov, and P. M. Echenique, Surf. Sci. **523**, L47 (2003).
- [37] H. L. Skriver and I. Mertig, Phys. Rev. B **41**, 6553 (1990).
- [38] M. Wulff, G. G. Lonzarich, D. Fort, and H. L. Skriver, Europhys. Lett. **7**, 629 (1988).